An *ab Initio* Study of D/H Exchange between CD_4 and the H-Forms of Zeolites FAU and MFI

G. J. Kramer*,† and R. A. van Santen†,‡

Contribution from the Koninklijke/Shell-Laboratorium, Amsterdam (Shell Research B.V.), P.O. Box 38000, 1030 BN Amsterdam, The Netherlands, and Schuit Institute of Catalysis, Eindhoven University of Technology, P.O. Box 513, 5600 MB Eindhoven, The Netherlands

Received May 4, 1994®

Abstract: D/H exchange between methane and a zeolite is the simplest reaction between a zeolitic proton and a hydrocarbon. Because of its simplicity, it offers a unique opportunity to test out possibilities that are offered by present-day computational techniques to obtain theoretical insight into the catalytic action of zeolites and to test theory against experiment. We report the results of an *ab initio* quantum chemical study of the D/H exchange process between CD_4 and a zeolitic cluster. Within this framework, a relation is established between acidity and the height of the barrier for exchange. This allows for the estimation of differences in the exchange barrier between various zeolites, of which HY (FAU) and HZSM-5 (MFI) are explicitly considered. Transition state theory is used to quantitatively predict the rate constant of the exchange process. The results compare favorably with D/H exchange experiments that have recently been performed.

1 Introduction

Conversion of hydrocarbons in zeolites, functioning as solid acid catalysts, is widely used in the chemical and petrochemical industries. Understanding of the catalytic process at the molecular level is considered an important aid in the area of catalyst research and development. The tremendous increase in computing power of recent years allows us to complement experimental results with accurate *ab initio* quantum chemical calculations on realistic model systems (see, *e.g.*, the review by Sauer[1]). The level of detail of the information contained in these theoretical results greatly facilitates the interpretation of experimental results.

In this paper we study theoretically the simplest reaction between a hydrocarbon and an H-zeolite, namely the exchange of hydrogen between methane and the zeolites HY (Faujasite or FAU) and HZSM-5 (or MFI), which are both well-studied but crystallographically very different zeolites. The chemical activation of CH_4 by a zeolitic proton can be considered a prototype for the activation of larger hydrocarbons *via* carbonium ion formation. Such positively charged carbonium ions with pentacoordinated carbon atoms have been postulated to be intermediate in monomolecular cracking reactions.[2,3] The proton exchange reaction of methane can be probed experimentally by isotope-labeling of either methane or the zeolite, as in

$$CD_4 + HZ \rightarrow CD_3H + DZ \qquad (1)$$

where HZ denotes a zeolite with an acidic OH group.

Given the supposed acid character of the process, a theoretical treatise of the exchange reaction requires knowledge about the proton affinities of different oxygen atoms in these two zeolites for which theoretical predictions have recently become available.[4−6] In these studies, proton affinities were computed using lattice energy calculations that are based on classical two- and three-body interaction potentials deduced from quantum chemical cluster calculations.[7] The use of classical force fields in these calculations allows one to include the effects of lattice relaxation upon (de)protonation, as well as that of long-range electrostatic interactions. The importance of including both of these effects is well documented.[8−10]

In order to correctly predict the energy for proton transfer between a zeolite and a basic molecule, *ab initio* cluster calculations have shown[11−13] that a combined geometry-optimization of the zeolite *and* sorbed molecule is essential in order to obtain a proper balancing of the energy cost of charge separation and that inclusion of the energy gained by "zwitterionic" interaction is essential. Because of this geometry-optimization requirement, the formation of a carbocationic carbonium ion from methane, *i.e.*, the transition state of the exchange process, can only be studied within the *ab initio* approximation by using the zeolite cluster approximation.

The work to be presented here provides a synthesis of the two extreme approaches, *i.e.*, between the quantum chemical cluster approximation and the classical lattice energy approximation. A brief summary of this work has been presented earlier.[14] Here, we give a more detailed account of the way in which the theoretical results were derived.

† Koninklijke/Shell-Laboratorium.
‡ Eindhoven University of Technology.
® Abstract published in *Advance ACS Abstracts*, February 1, 1995.

(1) Sauer, J. *Chem. Rev.* **1989**, *89*, 199.
(2) Haag, W. O.; Dessau, R. M. *Proc. 8th Int. Conf. Catal. West Berlin* **1984**, *2*, 305.
(3) Haag, W. O.; Lago, R. M.; Weisz, P. B. *Nature* **1984**, *309*, 589.
(4) Schröder, K.-P.; Sauer, J.; Leslie, M.; Catlow, R. C. A.; Thomas, J. M. *Chem. Phys. Lett.* **1992**, *188*, 320.
(5) Schröder, K.-P.; Sauer, J.; Leslie, M.; Catlow, R. C. A. *Zeolites* **1992**, *12*, 20.
(6) Kramer, G. J.; van Santen, R. A. *J. Am. Chem. Soc.* **1993**, *115*, 2887.
(7) Kramer, G. J.; de Man, A. J. M.; van Santen, R. A. *J. Am. Chem. Soc.* **1991**, *113*, 6435.
(8) Sauer, J.; Kölmel, C.; Hill, J.-R.; Ahlrichs, R. *Chem. Phys. Lett.* **1989**, *164*, 193.
(9) Nicholas, J. B.; Winans, R. E.; Harrison, R. J.; Iton, L. E.; Curtiss, L. A.; Hopfinger, A. J. *J. Phys. Chem.* **1992**, *96*, 10247.
(10) Cook, S. J.; Chakraborty, A. K.; Bell, A. T.; Theodorou, D. N. *J. Phys. Chem.* **1993**, *97*, 6679.
(11) Teunissen, E.; van Duyneveldt, F. B.; van Santen, R. A. *J. Phys. Chem.* **1992**, *96*, 366.
(12) Teunissen, E.; van Santen, R. A.; Jansen, A. P. J.; van Duyneveldt, F. B. *J. Phys. Chem.* **1993**, *97*, 203.
(13) Kassab, E.; Farquet, J.; Allevena, M.; Evleth, E. M. *J. Phys. Chem.* **1993**, *97*, 9034.

0002-7863/95/1517-1766$09.00/0

In section 2 we present the results of quantum chemical calculations of the exchange process between CD_4 and a zeolitic cluster. Special attention is given to the simulation of differences in proton affinity in these clusters, thereby establishing a connection between the zeolite cluster and the actual zeolite, where the variation in proton affinity (or acidity) is one of the reasons for the variation in reactivity observed in different types of zeolites. In section 3, the results of the quantum chemical calculations are used as input to calculate the exchange rate using transition state theory. In section 4, we quantify the differences in reaction rate between the zeolites FAU and MFI, taking differences in proton affinity and steric accessibility of the reaction site explicitly into account. Also, an upper limit to the exchange rate in any acidic aluminosilicate is given. The final sections are reserved for comparison with the experimental data (section 5) and for concluding remarks (section 6).

2. *Ab Initio* Quantum Chemical Calculations on the D/H Exchange between Methane and a Zeolitic Cluster

In this section, we will discuss the geometry of the minima and transition state along the reaction pathway for D/H exchange, the corresponding reaction barrier and its dependence on the basis set and size of the zeolite cluster (subsection 2.1), and the relationship between the reaction barrier and proton affinity (or acidity) of the zeolite cluster (subsection 2.2).

As the distinction between the hydrogen isotopes is irrelevant for all aspects of the calculations—except for the determination of vibrational frequencies—we will usually not explicitly mention the isotope.

2.1. The Exchange Path. In all our quantum chemical calculations, the infinite zeolite lattice is represented by a small "zeolitic" cluster: either the trimer $H_3SiO(H)Al(OH)_2OSiH_3$ or the monomer $HO(H)Al(OH)_3$ in which the two terminal SiH_3 groups have been replaced by hydrogen atoms. The molecular system used in the calculations consists of one of these zeolitic clusters and a methane molecule.

Figure 1A shows the geometry-optimized structure corresponding to the adsorption minimum of methane and the zeolite cluster. This minimum is taken to obey C_s symmetry, with the mirror plane defined by the plane of Si−**O**(H)−Al−**O**−Si (H−O(H)−Al−O−H for the monomer[15]).

Three possible transition state geometries were tested by quantum chemical geometry optimization using different starting geometries with different geometrical constraints. The optimized structures are shown in parts B−D of Figure 1. For the standard 3-21G basis set, the corresponding energies are listed in Table 1. Clearly, the exchange path where two different oxygen atoms are involved (B) is favored over the one that involves just a single oxygen atom (C). Likewise, transition state B is favored over a transition state where the CD_3 fragment resembles the ionic C_{3v}-symmetric conformation (D). This clear energetic preference proves the D/H exchange procees *via* transition state B. The same transition state is also reported in a recent paper by Evleth *et al.*[16] In what follows we will use that transition state conformation.

The transition state has a new plane of symmetry, perpendicular to that of the minimum; the mirror symmetry in this plane is lost in the transition state due to the 60° rotation of the CH_3 fragment. However, as this symmetry-breaking involves only the CH_3 fragment, we have chosen to retain this geometrical symmetry for the zeolite fragment.

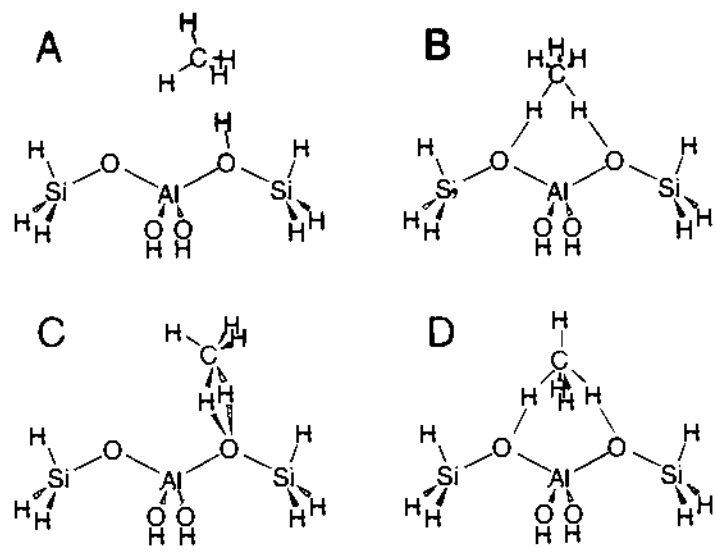

Figure 1. Molecular systems used in the quantum chemical calculations, consisting of a zeolite trimer and a methane molecule in an adsorption minimum (A), and in the transition state for exchange (B). Conformations C and D represent transition state geometries of exchange pathways with a markedly higher barrier energy. For conformations A, C, and D the Si−O−Al planes are symmetry planes; conformations B and D are mirror symmetric in a perpendicular plane through the $Al(OH)_2$ groups.

Table 1. Energies of the Geometry-Optimized Minimum and Various Transition State Geometries in the 3-21G Basis Set[a]

conformation	E (au)	B_0^0 (eV)
A (minimum)	−1158.70076	
B (transition state)	−1158.63061	1.91
C (transition state)	−1158.56490	3.70
D (transition state)	−1158.57118	3.53

[a] Conformation A through D are shown in Figure 1. B_0^0 is the barrier height of the symmetrical cluster equal to the energy difference between the minimum and the transition state.

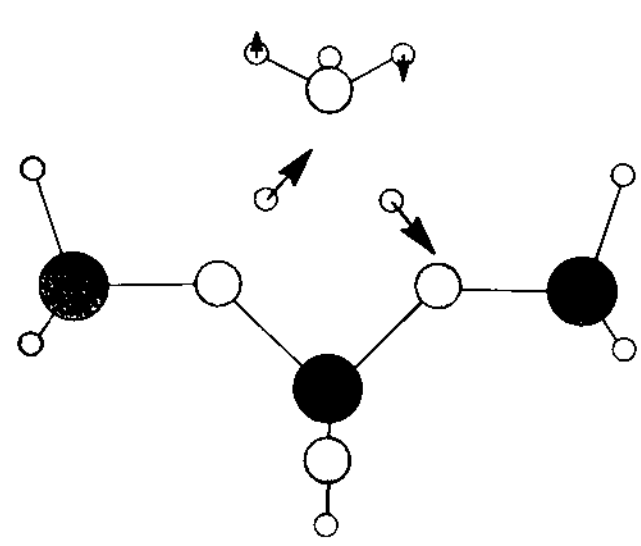

Figure 2. Reaction coordinate for the D/H exchange in the transition state based on vibrational analysis at the 3-21G-SCF level.

Proof that a molecular structure represents a transition state is provided by a vibrational analysis of the structure. Ideally, a minimum-energy structure has positive vibrational frequencies only, while a transition state has one negative (imaginary) frequency, corresponding to the reaction coordinate. A detailed discussion of the vibrational spectra is given in section 3. It suffices at this point to mention that the eigenmode associated with the imaginary frequency, as shown in Figure 2, is the proper reaction coordinate for D/H exchange involving two oxygen sites.

Both the minimum and transition state have been subjected to geometry optimization in a number of basis sets of increasing quality (3-21G, 3-21G**, and 6-31G**) at the self-consistent

(14) Kramer, G. J.; van Santen, R. A.; Emeis, C. A.; Nowak, A. K. *Nature* **1993**, *363*, 529.

(15) The C_s symmetric cluster is not the global energy minimum of these clusters. This would require C_1 symmetry, allowing for relative rotation of the terminal SiH_3 and OH groups. As these groups do not take part in the exchange process, this is a valid approximation.

(16) Evleth, E. M.; Kassab, E.; Sierra, L. R. *J. Phys. Chem.* **1994**, *98*, 1421.

Table 2. Total Energies of the Zeolite/Methane System at Different Levels of Computational Sophistication

cluster	basis set	method	minimum (au)	TS (au)	B_0^0 (eV)
trimer	3-21G	(SCF)	−1158.7008	−1158.6306	1.909
trimer	3-21G**	(SCF)	−1159.1277	−1159.0453	2.242
trimer	6-31G**	(SCF)	−1164.9129	−1164.8228	2.451
monomer	3-21G	(SCF)	−581.4964	−581.4363	1.633
monomer	3-21G**	(SCF)	−581.7242	−581.6466	2.110
monomer	6-31G**	(SCF)	−584.6782	−594.5913	2.365
monomer	3-21G	(SDCI)	−582.1230	−582.0721	1.385
monomer	3-21G**	(SDCI)	−582.7209	−582.6607	1.637
monomer	6-31G**	(SDCI)	−585.6830	−585.6166	1.806

Table 3. Mulliken Overlap Population for Minimum and Transition State Geometries[a]

		3-21G basis set		6-31G** basis set	
	bond	min.	TS	min.	TS
C−H	methane	0.37 (4×)	0.35 (3×)	0.40 (4×)	0.38 (3×)
C−H	exchanging H		0.128 (2×)		0.224 (2×)
O−H	exchanging H	0.247	0.140 (2×)	0.304	0.050 (2×)
Al−O	protonated O	0.085	0.126	0.071	0.154
Al−O	regular O	0.126	0.229	0.154	

[a] In the minimum, hydrogen is bonded to only one of the oxygen atoms; in the transition state, two exchanging hydrogen atoms are loosely bonded to two oxygen atoms of the zeolite cluster.

Table 4. Distances for the Minimum and Transition State Configurations

		minimum			transition state		
		3-21G	3-21G**	6-31G**	3-21G	-321G**	6-31G**
Al−O	protonated O	1.867	1.935	1.942	1.797	1.804	1.801
Al−O	regular O	1.709	1.714	1.706			
average		1.788	1.825	1.824	1.797	1.804	1.801
Si−O	protonated O	1.715	1.682	1.701	1.692	1.642	1.647
Si−O	regular O	1.638	1.613	1.615			
average		1.677	1.648	1.658	1.692	1.642	1.647
O−H	exchanging H	0.970	0.951	0.949	1.158	1.309	1.399
C−H	exchanging H				1.505	1.337	1.282

field (SCF) level. To check the influence of cluster termination, additional calculations have been performed on monomer clusters. Because of their reduced size, single−double configuration interaction calculations (SDCI) are possible and give an indication of the influence of correlation on the barrier height. The results are given in Table 2. There are systematic variations which are of some interest: the barrier increases upon the extension of the basis set and decreases significantly when correlation effects are taken into account. The influence of variation of the cluster size is relatively minor. Because SDCI covers only part of the correlation energy,[17] we estimate the proper value for the exchange barrier to be 1.6 ± 0.3 eV.

At first glance, the transition state seems to resemble a CH_5^+ ion close to the zeolite cluster. However, inspection of the overlap populations of the various bonds in the cluster (Table 3) reveals that the transition state is covalently bonded rather than ionically bonded. Significant features are the halving of the OH and CH overlap population for the hydrogen atoms transferring between the minimum and transition state and the invariance of the sum of the overlap populations between Al and the two oxygen atoms involved in the exchange.

The interatomic distances tabulated in Table 4 corroborate the idea of exchange as a covalent process. They show that, in the transition state geometry, the average Al−O bond length is

(17) Szabo, A.; Ostlund, N. S. *Modern Quantum Chemistry: Introduction to Advanced Electronic Structure Theory*; MacMillan: New York, 1982.

Table 5. Total Energies of the Zeolite/Methane System at Different Levels of Computational Sophistication[a]

distance Si−H (Å)	Z^-	ZH	minimum	transition state
		3-21G Basis Set		
1.30	−1118.0819	−1118.6245	−1158.6029	−1158.5358
1.40	−1118.1682	−1118.7038	−1158.6822	−1158.6140
1.50	−1118.1920	−1118.7203	−1158.6986	−1158.6294
1.70	−1118.1318	−1118.6458	−1158.6240	−1158.5533
1.90	−1118.0045	−1118.5061	−1158.4841	−1158.4148
		6-31G** Basis Set[b]		
1.50	−1124.0159	−1124.5473	−1164.7501	−1164.6625
1.70	−1123.9634	−1124.4794	−1164.6822	−1164.5954

[a] The data have been used to calculate the barrier heights used in Figure 3. Energy units are in au. [b] Polarization functions have been added to the CH_5 fragment and two oxygen atoms only.

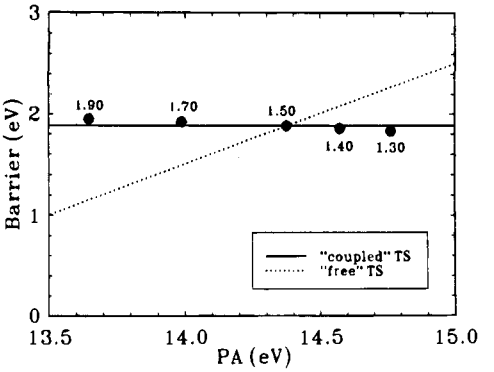

Figure 3. Variation of the proton exchange barrier with proton affinity of the zeolite cluster. The numbers refer to the Si−H distance within the SiH_3 groups. The interpretation of the terms "free TS" and "coupled TS" is discussed in the text.

equal to that in the minimum. For a negatively charged zeolite cluster one would expect somewhat shorter Al−O bond lengths. Also, the exchanging hydrogen atoms are in between the oxygen and carbon atoms at roughly equal bonding distances, although there is a considerable change in the hydrogen bond lengths upon addition of polarization functions.

2.2. Relation between Reaction Barrier and Proton Affinity. In the above, we have represented the infinite zeolite by a small, zeolitic cluster. Since our main interest is in reactions in zeolites, which are extended systems of considerable heterogeneity, we have to take the heterogeneous nature of zeolites and of zeolite acidity into account. To this end, we focus on nonideal clusters in which the influence of an extended lattice on local properties, specifically acidity, can be studied.

In an earlier work[6] we showed that the proton affinity of zeolites, which is the theoretical measure of zeolite acidity, is modified by both chemical and structural variations in the zeolite lattice. In the same reference, it was shown that the variation in proton affinity may be mimicked by constraining the peripheral bonds of the zeolite cluster. By assignment of different bond lengths to the terminal Si−H bonds in subsequent calculations, the proton affinity may be varied over a range of 1−2 eV, which is of the same order of magnitude as the expected variation in zeolites.

Table 5 and Figure 3 show the dependence of the exchange barrier on changes in the proton affinities of *both* oxygen sites involved. As indicated before, the proton affinities were varied by adjusting the Si−H bond length of the peripheral groups. All other geometric degrees of freedom were optimized. As can be seen from the figure, the barrier (B_0, in eV) is only weakly dependent on the proton affinity (PA or $\mathscr{P}$):

$$B_0 = 1.865 - 0.109(\mathscr{P} - 14.47) \quad (2)$$

Here, 14.47 eV is taken as a reference point for the proton affinity.

We have also investigated the dependence of the barrier height on proton affinity *differences*: the proton affinities of the two oxygen sites involved were made nonequivalent by setting the terminal bond lengths of the two SiH_3 groups to different values. The resulting loss of symmetry required a different search method for optimization of the transition state from that for the symmetric case. This required more computing time but yielded results of the same quality. Figure 4 shows the result, based on the energy data given in Table 6. Correcting these values for the weak dependence of B on $\mathscr{P}$ (eq 2), we find a clear dependence of B on the proton affinity *difference* ($\delta\mathscr{P}$):

$$B_0 = 1.865 + 0.72|\delta\mathscr{P}| \quad (3)$$

Note that the barrier is always expressed relative to the minimum with the lowest energy, *i.e.*, by the proton attached to the oxygen site with the highest proton affinity.

We have verified that these results, which were obtained at the 3-21G level, are essentially retained when using a larger (6-31G**) basis set. Data are given in Table 6. The results with this basis set are described by

$$B_0 = 2.385 + 0.06(\mathscr{P} - 14.47) \quad (4)$$

$$B_0 = 2.385 + 0.6|\delta\mathscr{P}| \quad (5)$$

In later sections we will neglect the (weak) dependence of the barrier on the proton affinity and use

$$B_0 = B_0^0 + \mathscr{G}|\delta\mathscr{P}| \quad (6)$$

where B_0^0 denotes the energy difference between the sorption minimum and the transition state, estimated as 1.6 ± 0.3 eV. The constant of proportionality between barrier and proton affinity *differences* ($\mathscr{G}$) is approximately 0.7.

The rationale behind the dependence of the exchange barrier on proton affinity *differences*, rather than on the proton affinity itself, is the retention of covalent bonding between methane (or the CH_5 fragment) and the zeolite in the transition state. Figure 5 shows the expected dependencies for an ionic transition state, one that is completely decoupled from the zeolite cluster ("free"), and for a transition state which retains the covalent bonding of acid hydrogen with the zeolite ("coupled"). In the first case, the transition state energy is unaffected by the proton affinity of either of the oxygen atoms. In the "coupled" case, the transition state energy level should be determined by the average proton binding strength of both oxygen atoms.

It is important to note that in the case where the two oxygen atoms have different proton affinities, the activation energy of the exchange process is determined by the barrier measured with repect to the minimum of lowest energy, *i.e.*, where the proton is bonded to the oxygen atom with the highest proton affinity. For the reverse exchange path, the activation energy is smaller by an amount $\delta\mathscr{P}$, and the population of that oxygen site is smaller by a factor $\exp(-\delta\mathscr{P}/kT)$, canceling the effect of the lower activation energy. In this situation, it is assumed that there is thermal equilibrium between the proton population of both oxygen sites. This is indeed the case; according to Sauer *et al.*,[18] the barrier for direct proton exchange between neighboring oxygen sites is only 0.5 eV, much lower, and thus the exchange much faster, than that for the presently discussed process.

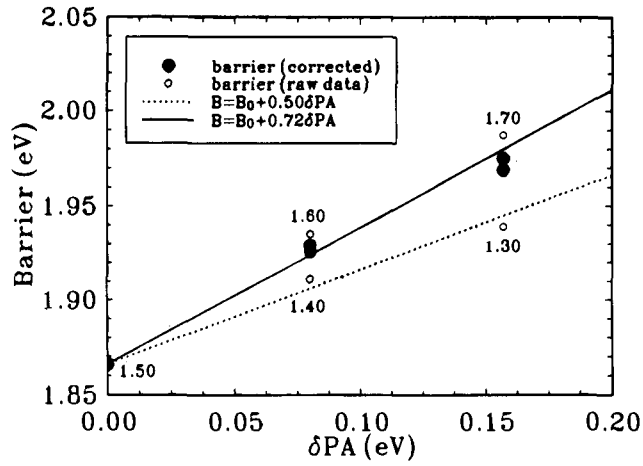

Figure 4. Variation of the proton exchange barrier with proton affinity *differences* between the two oxygen sites of the zeolite cluster. Numbers in the figure refer to the Si−H distance within one of the SiH_3 groups. The distances in the other are kept at 1.50 Å. The correction of the data is discussed in the text.

3. Transition State Theory of the D/H Exchange Reaction

In this section we explicitly calculate the D/H exchange rate from semiclassical transition state theory, using on *ab initio* quantum chemical data. For the details of the theory we refer to Glasstone[19] and Rice.[20] The D/H exchange reaction is between deuterated methane and a protonated zeolite (HZ)

$$CD_4 + HZ \underset{k_f}{\overset{k_b}{\rightleftharpoons}} CD_3H + DZ \xrightarrow{k_2} \ldots \quad (7)$$

with k denoting the rate constants. When diffusion is fast and there is an excess amount of CD_4, the backward reaction, as well as any further reactions of CD_3H, may be neglected ($k_b = k_2 \approx 0$). The D/H exchange rate (r_f) is thus

$$r_f = -\frac{d[HZ]}{dt} = k_f[HZ][CD_4] \quad (8)$$

We will consistently express concentrations in m^{-3} rather than in $mol \cdot m^{-3}$. The exchange reaction will proceed from an initial state (CD_4 + HZ), via an *activated complex*, to a final state (CHD_3 + DZ). Within the framework of transition state theory, *i.e.*, assuming thermodynamic equilibrium between the initial state and the activated complex and separability of the reaction coordinate, the exchange rate can be expressed as a product of partition functions (Π)

$$r_f = \frac{k_B T V}{h} \frac{\Pi'_{TS}}{\Pi_{CD_4}\Pi_{HZ}}[HZ][CD_4] \quad (9)$$

where the subscript TS refers to the transition state complex, HZ to the zeolite cluster, and the prime indicates that the reaction coordinate is not considered in the evaluation of the transition state partition function. V is the volume of the system. We emphasize that in calculating Π_{HZ} the precise definition of "HZ"

(18) Sauer, J.; Kölmel, C. M.; Hill, J.-R.; Ahlrichs, R. *Chem. Phys. Lett.* **1989**, *164*, 193.

(19) Glasstone, S. *Theoretical Chemistry*; Van Nostrand: New York, 1944.

(20) Rice, O. K. *Statistical Mechanics, Thermodynamics, and Kinetics*; Freeman: San Francisco, 1966.

Table 6. Total Energies of the Zeolite/Methane System at Different Levels of Computational Sophistication[a]

distance (Si−H) (Å)	Z^-	$ZH_{1.50}$	ZH_{var}	$minimum_{1.50}$	$minimum_{var}$	transition state
			3-31G Basis Set			
1.30	−1118.1370	−1118.6696	−1118.6754	−1158.6478	−1158.6538	−1158.5826
1.40	−1118.1801	−1118.7106	−1118.7135	−1158.6888	−1158.6919	−1158.6217
1.60	−1118.1834	−1118.7096	−1118.7066	−1158.6879	−1158.6848	−1158.6168
1.70	−1118.1620	−1118.6860	−1118.6803	−1158.6644	−1158.6583	−1158.5913
			6-31G** Basis Set[b]			
1.70	−1123.9898	−1124.5164	−1124.5104	−1164.7193	−1164.7129	−1164.6287

[a] The clusters are asymmetric. The Si−H bonding distance in one of the terminal groups has been fixed at 1.5 Å; the other is varied as indicated in the first column. $ZH_{1.50}$ denotes the configuration where the proton resides on the side of the SiH_3 group with 1.5 Å bonding distances. The other subscripts can be similarly understood. The data have been used to calculate the barrier heights used in Figure 4. Energy units are in au. [b] Polarization functions have been added to the CH_5 fragment and two oxygen atoms only.

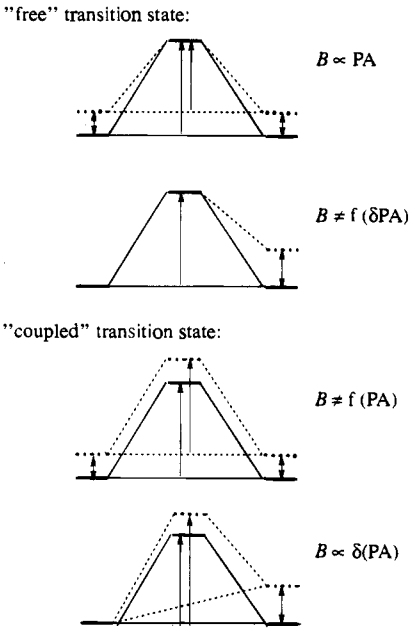

Figure 5. "Free" and "coupled" transition states. In the transition state, covalent bonding between the zeolite and the exchanging protons is retained. As a consequence, the reaction barrier (B) is independent of the proton affinity itself (above) but dependent on PA differences (below).

is irrelevant since only the ratio Π'_{TS}/Π_{HZ} appears in the expression for the exchange rate. From a molecular viewpoint, it is evident that extension of a zeolite cluster does not affect the result since additional degrees of freedom cancel each other in Π'_{TS}/Π_{HZ}. Obviously, explicit calculations should be based on a zeolite fragment of such size that its termination does not affect the transition state in any way other than for the minimum energy configuration.

So far we have not been explicit about the nature of the initial state. We have implicitly used a molecular picture where collisions between methane and a HZ "molecule" lead to exchange reactions. In reality, methane from the gas phase first has to be adsorbed into the zeolite pores, and only then can it exchange one of its hydrogen atoms with one of the zeolite's acid groups. However, this pre-equilibrium does not change the expression for the rate constant. If the adsorption step is explicitly accounted for, the rate constant becomes the product of the equilibrium constant for adsorption and the rate constant for exchange from the adsorption complex. The first is directly proportional to the partition function of the adsorption complex, while the latter is inversely proportional to it, which cancels their contribution to the product. In physical terms the experimental condition of constant gas pressure implies that the gas phase is the reference point for all calculations and that the intermediate state drops out of the equations.

3.1. Vibrational Spectrum of the Initial State and of the Transition State. As is clear from the above discussion of transition state theory, the explicit calculation of rate constants requires knowledge of all excited states of both the minimum and transition state in order to evaluate the partition sum. It is known that *ab initio* calculations overestimate vibrational frequencies systematically by approximately 10%.[21] However, this overestimation does not have a major effect on the calculated rate constants, and no "corrections" have been applied to the directly calculated frequencies.

At the 3-21G-SCF level we have determined the vibrational spectrum of the minimum (the absorption complex) and the transition state from the computed matrix of second derivatives of the energy with respect to the atomic coordinates. The atomic weights of the hydrogen atoms have been taken as required for the specific D/H exchange process

$$CD_4 + HZ \rightarrow CD_3H + DZ \qquad (10)$$

A list of the frequencies is given in Table 7, and a graphic representation is shown in Figure 6 where all 57 modes of vibration are separated according to their nature. It appeared that all modes could be unambiguously assigned to either the zeolite cluster, to CD_4, or to the acidic OH bond. When minimum and transition state modes are compared, differences will be expected mainly in the latter two categories. Indeed, all 39 modes that are ascribed to the zeolite—excluding the acid OH vibrational modes—are at approximately the same frequency for the minimum and for the transition state. Assignment of "HZ" modes is as follows: modes below 1300 cm^{-1} are SiO/AlO vibrational modes, similar to those observed in zeolites, and modes around 2300 and 4100 cm^{-1} are terminal OH and SiH stretch modes, respectively. There are a few modes with small negative frequency, as a spurious consequence of the C_s symmetry of the cluster. Since these modes correspond to rotation of terminal groups, they are of no consequence for the exchange process.

Important shifts occur in the OH and CD_4 frequencies (lower half of the figure). The OH stretch vibration (at 3890 cm^{-1}) disappears in the transition state and so do the six very low frequency modes that describe the loose coupling between methane and zeolite in the adsorption state. In their places, we find a large negative frequency (−1423 cm^{-1}) that corresponds to the reaction coordinate, and six modes between 20 and 710 cm^{-1} that describe the zeolite−CD_4H coupling in the transition state. The 20 cm^{-1} frequency corresponds to the rotation of the CD_3 group. For the minimum, the acid OH group has bending modes at 631 and 1212 cm^{-1}; nine other modes between 1200 and 2500 cm^{-1} are internal CD_4 modes. These

(21) Dijkstra, C. E. *Ab-initio Calculation of Structures and Properties of Molecules*; Studies in Physical and Theoretical Chemistry *58*; Elsevier: Amsterdam, 1988.

Table 7. *A Initio* Computed Vibrational Frequencies of the Absorption Minimum, the Transition State, and CD_4, as Used in the Evaluation of Partition Functions in Section 3.2[a]

minimum	transition state	CD_4	minimum	transition state
−200.414 (Z)	−1423.384 (RC)		922.909 (Z)	929.808 (Z)
−127.723 (Z)	−155.086 (Z)		992.409 (Z)	1000.625 (Z)
−56.788 (I)	−42.834 (Z)		1007.079 (Z)	1002.056 (Z)
−22.541 (Z)	20.055 (CD_4H)		1022.242 (Z)	1003.940 (Z)
−12.698 (Z)	65.281 (Z)		1022.491 (Z)	1015.540 (Z)
18.883 (Z)	75.525 (Z)		1024.563 (Z)	1024.511 (Z)
51.410 (I)	92.269 (Z)		1057.791 (Z)	1030.969 (Z)
60.951 (Z)	93.499 (Z)		1130.540 (Z)	1041.225 (Z)
70.932 (I)	111.747 (Z)	1150.520	1145.340 (CD_4)	1063.864 (Z)
78.377 (I)	119.427 (Z)	1150.521	1150.732 (CD_4)	1093.880 (CD_4H)
81.997 (Z)	136.486 (Z)	1150.522	1156.924 (CD_4)	1107.703 (Z)
88.801 (I)	210.284 (Z)		1212.098 (OH)	1169.646 (CD_4H)
108.067 (I)	235.131 (Z)	1230.855	1231.151 (CD_4)	1189.699 (CD_4H)
134.375 (Z)	244.802 (CD_4H)	1230.856	1232.189 (CD_4)	1321.381 (CD_4H)
172.870 (Z)	269.927 (Z)		1242.456 (Z)	1338.583 (CD_4H)
233.084 (Z)	281.693 (Z)		2238.790 (Z)	1411.162 (CD_4H)
245.355 (Z)	324.785 (CD_4H)	2253.197	2248.249 (CD_4)	1867.356 (CD_4H)
282.043 (Z)	354.233 (Z)		2249.304 (Z)	2269.701 (CD_4H)
329.364 (Z)	422.633 (CD_4H)		2287.565 (Z)	2313.684 (Z)
345.707 (Z)	444.253 (Z)		2327.121 (Z)	2314.238 (Z)
379.518 (Z)	456.203 (CD_4H)		2364.489 (Z)	2318.733 (Z)
547.412 (Z)	620.416 (Z)		2366.677 (Z)	2319.520 (Z)
570.468 (Z)	632.655 (Z)	2426.021	2414.908 (CD_4)	2333.209 (Z)
631.541 (OH)	710.453 (CD_4H)	2426.022	2423.958 (CD_4)	2334.734 (Z)
762.751 (Z)	787.758 (Z)	2426.023	2428.049 (CD_4)	2359.810 (CD_4H)
767.409 (Z)	792.867 (Z)		3889.813 (OH)	2394.199 (CD_4H)
823.778 (Z)	803.584 (Z)		4149.884 (Z)	4163.601 (Z)
829.068 (Z)	812.378 (Z)		4152.312 (Z)	4166.858
913.997 (Z)	894.133 (CD_4H)			

[a] The assignment of modes is discussed in section 3.1. Z is the zeolite, I is the intermolecular coupling between methane and zeolite, OH is the acid proton, CD_4 and CD_4H are the internal modes of the corresponding fragments, and RC is the reaction coordinate. Units are in cm^{-1}.

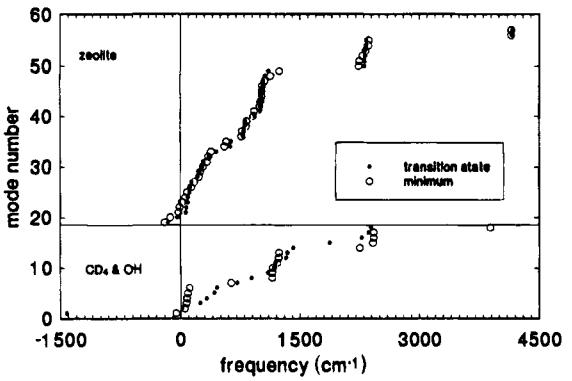

Figure 6. Computed vibrational frequencies for the adsorption minimum and transition state for D/H exchange. The assignment of modes is discussed in the text.

frequencies determine to a large extent the entropy reduction in the transition state and thereby the reaction probability. Below, we will discuss this point further.

As discussed above, the reference point for the calculation of the rate constant is the gas-phase CD_4 molecule. Its vibrational frequencies have been calculated separately at the same computational level (see Table 7); they do not differ much from the values obtained for the adsorption minimum where CD_4 is close to a zeolite cluster.

In assessing the dependence of reaction rate on zeolites (section 4) we will focus solely on variations in the exchange barrier. Since vibrational frequencies determine the pre-exponential factor of the reaction rate, it is worthwhile to check the extent to which these are influenced by proton affinity differences between sites. We compared the transition state vibrational frequencies of two clusters that have proton affinity differences of 0 and 0.08 eV, respectively. It was found that the six vibrational modes that account for the methane−zeolite coupling are the same to within 10 cm^{-1}.

3.2. Calculation of the Pre-exponential factor for D/H Exchange. We will now turn to the evaluation of partition sums in order to estimate the rate constant for D/H exchange according to eq 9. For a system with total energy levels ϵ_i of degeneracy g_i the partition function reads

$$\Pi = \sum_i g_i e^{-\epsilon_i/k_B T} \tag{11}$$

The total energy may be separated into terms corresponding to different degrees of freedom, such as translational, rotational, and vibrational ones:

$$\Pi = \Pi_{trans}\Pi_{rot}\Pi_{vib}e^{-E_0/k_B T} \tag{12}$$

We define E_0 as the ground state energy of the system, *excluding* zero-point contributions.

We recall that the quantum mechanical translational and vibrational partitions are given by

$$\Pi_{trans} = \frac{(2\pi m k_B T)^{1/2}}{h^3} V \tag{13}$$

$$\Pi_{vib} = \frac{e^{-(1/2)(h\nu/k_B T)}}{1 - e^{-h\nu/k_B T}} \tag{14}$$

where the factor $e^{-(1/2)(h\nu/k_B T)}$ contains the zero-point energy of a harmonic oscillator with frequency ν. The rotational partition function of CD_4 is that of a symmetric top molecule with three identical moments of inertia I_x[22]

(22) Davidson, N. *Statistical Mechanics*; McGraw-Hill: New York, 1962.

$$\Pi_{rot} = \frac{\pi^{1/2}}{\sigma}\left(\frac{8\pi^2 I_x k_B T}{h^2}\right)^{3/2} \quad (15)$$

where σ is the symmetry number, which equals 12 for CD_4. Using the *ab initio* geometry for CD_4, the numerical value for I_x is 5.23×10^{-47} kg·m^2.

The expression for the exchange rate (eq 9) may now be written as

$$r_f = \frac{k_B T V}{h}\frac{\Pi_{TS,trans}\Pi_{TS,rot}\Pi'_{TS,vib}}{\Pi_{CD_4,trans}\Pi_{CD_4,rot}\Pi_{CD_4,vib}\Pi_{HZ,trans}\Pi_{HZ,rot}\Pi_{HZ,vib}} \times [HZ][CD_4]e^{-B/k_BT}$$

$$= \frac{k_B T V}{h}\frac{\Pi'_{TS,vib}}{\Pi_{CD_4,trans}\Pi_{CD_4,rot}\Pi_{CD_4,vib}\Pi_{HZ,vib}}[HZ][CD_4]e^{-B/k_BT} \quad (16)$$

or simply

$$r_f = r_0 e^{-B/k_BT} \quad (17)$$

The translational and rotational partition functions of the zeolite and the transition state cancel each other because the real zeolite is an "infinite" system, even though this is not true for the zeolite cluster. B is the barrier height, which is formally equal to $E_{TS} - E_{CD_4} - E_{HZ}$. Note that the barrier as defined here does not contain the zero-point vibrations. These are contained in the prefactor r_0, which is the same for all zeolites. The only zeolite-dependence is contained in the barrier B.

On the basis of the vibrational data of the cluster calculations, $\Pi'_{TS,vib}$ includes 56 modes of the transition state cluster: 39 are zeolite modes and 18 stem from the CD_4H fragment. The reaction coordinate vibration is excluded. $\Pi_{CD_4,vib}$ contains 9 vibrations and $\Pi_{HZ,vib}$, 38. An additional six degrees of freedom are accounted for in $\Pi_{CD_4,trans}$ and $\Pi_{CD_4,rot}$. As indicated above, the vibrational modes of the zeolite are approximately the same in the minimum and in the transition state. Hence, their contribution cancels out in the rate expression. Thus, the only modes that need to be taken into account explicitly are those for CD_4 and OH.

So far, we have implicitly assumed a single transition state and a single minimum. For any acid $AlO_4(+H)$ tetrahedron the minimum (HZ) is 4-fold degenerate (four equal oxygen atoms) and the transition state, 6-fold (each of the six ribs of the tetrahedron may accommodate the transition state complex). However, when the tetrahedron is embedded in an infinite zeolite lattice, not all sides of the tetrahedron are accessible for methane. Hence, in practice this degeneracy is reduced to five. This point will be discussed further in section 4. Thus, when degeneracy is taken properly into account, eq 16 should be multiplied by $^5/_4$.

Together, the above allows us to evaluate r_0 numerically. Comparison of the results with experimental findings is deferred to section 5.

3.3. Quantum Corrections. The above treatment of the reaction rate is termed semiclassical since it is assumed that a reaction can take place only when the energy is greater than or equal to the barrier energy thereby neglecting the possibility of tunneling through the barrier. Since we are discussing exchange of protons, for which quantum effects are often important, we have estimated the quantum correction to the semiclassical results.

Following Johnston,[23] we have assumed that the reaction path is one-dimensional and consists of two semi-infinite stretches where the energy is constant (initial and final state), separated by a smooth potential barrier (transition state) of the so-called Eckart-type. Using the previously calculated values for the barrier height and the imaginary frequency of the reaction coordinate, we find only a moderate quantum correction to the reaction rate, varying between a factor of 2 at 500 K and 1.2 at 1000 K.

In conclusion, quantum corrections are not very large, indicating that even though we are dealing with hydrogen and deuterium, the system is essentially classical, and tunneling is not dominant.

3.4. Semiclassical Interpretation of the Transition State. The above calculation of reaction rates was rather formal, leaving little opportunity to check if results are chemically or physically "reasonable". A different approach to reaction rates is to start with the collision rate (r_0) between CD_4 and acid protons.[24]

$$r_0 = \sigma \bar{u}_s [HZ][CD_4] \quad (18)$$

Here σ is the collision cross section of CD_4 ($\approx$6 Å^2), and $\bar{u}_s$ is the average thermal velocity with which CD_4 hits the zeolite surface, which equals

$$\bar{u}_{CD_4} = \frac{1}{4}\sqrt{\frac{8k_BT}{\pi m_{CD_4}}} \quad (19)$$

Naturally, the reaction rate (r_f) is proportional to the product of the collision rate and the thermal probability of crossing the barrier:

$$r_f = P r_\sigma e^{-\tilde{B}/k_BT} \quad (20)$$

Here we have introduced $\tilde{B}$, which differs from B by the inclusion of zero-point vibrational energies. The constant of proportionality P is known as the steric factor and can be used to define the *reactive* crosssection σ^*:

$$\sigma^* = P\sigma \quad (21)$$

In general, P differs from unity as a consequence of entropy differences between the minimum and the transition state. Since the transition state entropy is usually reduced with respect to that of the minimum because of, *e.g.*, restricted rotational freedom, P is usually smaller than 1.

One can estimate σ^* (or P) by equating eq 20 with eq 16. At a typical reaction temperature (700 K), these equations give

$$r_\sigma = (2.2 \times 10^2)\sigma^*[HZ][CD_4] \quad (22)$$

and

$$r_\sigma = (1.5 \times 10^{-19})[HZ][CD_4] \quad (23)$$

respectively, from which it follows that σ^* is approximately 6.9×10^{-2} Å^2 and P, approximately 10^{-2}. Such a value is indicative of a so-called loose transition state, for which the reduction of rotational and vibrational entropy is relatively minor, and does not severely hinder the reaction.

4. Exchange in the H-Zeolites FAU and MFI

We now turn to the application of the above results to "real zeolites", specifically FAU and MFI, and quantify the differences between these zeolites in their capacity to exchange acid

(23) Johnston, H. S. *Gas Phase Reaction Rate Theory*; Ronald Press: New York, 1966.

(24) See, *e.g.*, Atkins, P. W. *Physical Chemistry*, 4th ed.; Oxford University: Oxford, 1990; Chapter 28.

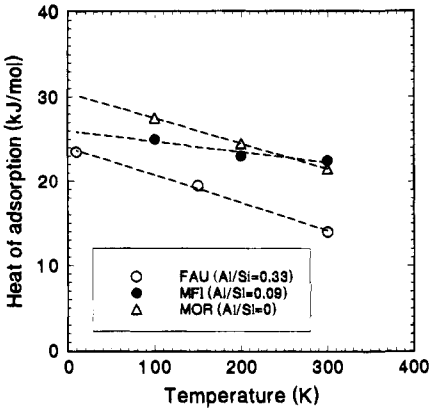

Figure 7. Calculated temperature dependence of the isosteric heat of adsorption in three different zeolites.[27]

hydrogen atoms with deuterated methane. As we have seen above, the zeolite dependence is contained in the effective barrier B that enters into the expression for the reaction rate:

$$B = E_{TS} - (E_{CD_4} + E_{HZ}) \tag{24}$$

or, equivalently

$$B = (E_{TS} - E_{AC}) - (E_{CD_4} + E_{HZ} - E_{AC}) \tag{25}$$

Here, the first term represents the activation energy from the adsorption complex (AC) to the transition state and is equivalent to B_0, which was introduced in the discussion of the cluster calculations (section 2); the second is the adsorption energy, Q_A. Its evaluation requires that we quantify (i) the varying acidity of the acid OH groups in real zeolites, which modifies $E_{TS} - E_{AC}$, and (ii) the adsorption energy. We start with the latter.

It is well known that *ab initio* quantum chemistry does not accurately predict adsorption energies. This is because adsorption energies are relatively small as well as being due to van der Waals and ionic interactions. The van der Waals interaction is neglected at the SCF level, and the long-range character of the ionic interactions (with methane's quadrupole moment and induced dipole moment) makes its value sensitive to cluster size. Hence, we will estimate Q_A for FAU and MFI from empirical data. The adsorption energies of methane in various zeolites are known both from experiment[25] and from molecular modeling.[26,27]

The isosteric heat of adsorption is a quantity that depends not only on zeolite type but also on pressure (loading) and temperature. It should be realized that the temperature-dependent heat of adsorption is actually the free energy of adsorption. From its introduction in the preceding section, it is evident that Q_A is the energy of adsorption in an adsorption minimum, which equals the isosteric heat of adsorption at zero temperature where there are no entropic effects.

As no low-temperature experimental adsorption data are available, we must rely on modeling results. In Figure 7 we have reproduced the data from Den Ouden,[27] showing the calculated, temperature-dependent heats of adsorption in FAU and MFI. It is seen that the heats of adsorption of FAU and MFI extrapolate to similar values. The values are even closer if we take the difference in Al/Si ratio into account. In his study, the author found that the heat of adsorption increases by around 10% if the Al/Si ratio of FAU is lowered from 0.33 to zero. Thus for both FAU and MFI, 0.26 eV is the best estimate for Q_A.

4.1. Influence of Acidity on the Reaction Rate. In a previous paper[6] we have estimated the proton affinity differences between all crystallographically different sites in FAU and MFI. In order to estimate the effective reaction rate in either of these zeolites, we will consider (i) all possible combinations of two oxygen sites, (ii) the possible steric hindrance of the exchange, and (iii) quantification of the effects of proton affinity differences on the reaction rates for those reaction paths that are sterically accessible.

At this stage it is useful to introduce the concept of an "ideal zeolite". As we have seen, the reaction barrier is lowest if the proton affinities of the two oxygen sites involved are equal. A lower bound to the barrier provides an upper bound to the reaction rate. Similarly, exclusion on steric grounds of reaction pathways that involve certain pairs of oxygen atoms reduces the reaction rate in real zeolites. An "ideal zeolite" is so defined as to suffer as little as possible from steric hindrance. While an AlO_4 tetrahedron has six oxygen–oxygen ribs that may provide a reaction path, the embedding of the tetrahedron in an infinite structure will always cause at least one of these ribs to be "inside" the zeolite framework and therefore to be inaccessible to reactant molecules. Thus, the "ideal zeolite" is defined as having five reaction pathways per aluminum tetrahedron. Below, we express the reaction rates of FAU and MFI as fractions of the reaction rate in the "ideal zeolite". Thereby, the "ideal zeolite" provides a useful reference point for the comparison of reaction rates in zeolites with that in the molecular model system.

As we have seen (eq 6), the barrier B is dependent on differences in proton energy ($\mathcal{E}$, defined as the negative of the proton affinity) between oxygen sites j and k

$$B_0 = B_0^0 + \mathcal{C}|\mathcal{E}_k - \mathcal{E}_j| \tag{26}$$

The proton occupancy n of sites will obey a Boltzmann distribution

$$n_j = \frac{\exp(-\mathcal{E}_j)}{\sum_i \exp(-\mathcal{E}_i)} \tag{27}$$

when proton equilibration is fast compared to the D/H exchange reaction. This is indeed the case; *ab initio* calculations[18] indicate that the barrier for direct proton transfer is approximately 0.5 eV, which is much lower than the D/H exchange barrier.

With these definitions, the reaction rate (eq 17) can be generalized to describe the effect rate constant in a zeolite with different T-sites (numbered I). The "reaction rate", or more accurately, the rate at which acid hydrogen is replaced by deuterium, is an average over all T-sites and over all available reaction paths, giving

$$r_f = r_0(T)\exp[-(B_0^0 - Q_A)/k_BT]\sum_I \sum_{j,k:\mathcal{E}_j<\mathcal{E}_k} f_I n_j^I \times \exp(-\mathcal{C}(\mathcal{E}_k - \mathcal{E}_j)/k_BT) \tag{28}$$

Here, f_I is the fraction of crystallographic T-sites that are of type I, and j and k run over the oxygen sites of the AlO_4 tetrahedron. The reaction rate expression can be split into a zeolite-independent part $\mathcal{R}_0(T)$ and a zeolite-dependent part $\mathcal{F}(T)$

(25) Barrer, R. M.; Sutherland, J. W. *Proc. R. Soc. London, A* **1956**, *237*, 439. Papp, H.; Hinsen, W.; Do, N. T.; Baerns, M. *Thermochim. Acta* **1984**, *82*, 137.

(26) Yashonath, S.; Thomas, J. M.; Nowak, A. K.; Cheetham, A. K. *Nature* **1988**, *331*, 601.

(27) Den Ouden, C. J. J., Ph.D. Thesis; University of Eindhoven, 1992.

$$r_f = \mathcal{R}_0(T)\mathcal{F}(T) \quad (29)$$

$$\mathcal{R}_0(T) = r_0 \exp[-(B_0^0 - Q_A)/k_B T] \quad (30)$$

$$\mathcal{F} = \sum_I \sum_{j,k:\mathcal{E}_j<\mathcal{E}_k} f_I n_j^I \exp(-\mathcal{C}(\mathcal{E}_k - \mathcal{E}_j)/k_B T) \quad (31)$$

Note that $\mathcal{R}_0(T)$ is the rate constant of the "ideal zeolite", and $\mathcal{F}(\leq 1)$ is the activity of a particular zeolite relative to that of the "ideal zeolite".

4.1.1. Faujasite. The proton affinities in zeolite FAU have been calculated previously.[6] The four oxygen sites surrounding the one unique T-site have proton energies as listed in Table 8. Out of the hypothetical six pathways, only the three that involve oxygen sites 1, 2, and 4 are available for D/H exchange because for these positions the proton protrudes into the supercage of the faujasite structure. Protons attached to O_3 protrude into the small sodalite cage. Although methane cannot pass into this cage, construction of a transition state geometry that uses O_3 proves sterically impossible.

In principle this information suffices to calculate the reaction rate in FAU. However, since it has a simple crystal structure and has been studied extensively over the years, we have information about the relative proton population of the oxygen sites. X-ray studies[28] have revealed that usually sites 1 and 3 are occupied to a similar extent, whereas, based on a Boltzmann distribution between sites that differ by 0.2–0.5 eV in energy (Table 8), one would expect at least a 1:10 population ratio between them. This apparent contradiction is resolved by the notion—from experimental work—that the O_3 proton population is restricted. O_3 protons of different AlO_4 tetrahedra would be too close together, which restricts the O_3 population when the aluminum content is significant. Excess protons then populate site 1. In the sample used for the D/H exchange experiment, one-third of the protons reside on O_3 and are inactive; the remainder are on the other sites and are responsible for D/H exchange. Taking all experimental and theoretical information into account we have

$$\mathcal{F}_{FAU} = 0.67 \sum_{j,k:\mathcal{E}_j<\mathcal{E}_k}^{\{1,2,4\}} \exp[-\mathcal{C}(\mathcal{E}_k - \mathcal{E}_j)]/ \sum_j^{\{1,2,4\}} \exp(-\mathcal{E}_i) \quad (32)$$

The numerical values of $\mathcal{F}_{FAU}$ vary (within the experimentally accessible temperature range) between 0.007 at 350 °C and 0.0016 at 480 °C.

4.1.2. ZSM-5 or MFI. Previous work[6] has provided estimates for the proton energies of all 48 possible combinations of proton and aluminum substitutions in MFI. Although different force fields produced different estimates for the magnitude of proton energy differences, the relative order of proton energies was consistently reproduced with all force fields. In addition, we have expressed the relative proton energy in terms of the width of the distribution. The width is somewhat uncertain but estimated to be between 0.6 and 0.8 eV. The data (which were presented in a graph in ref 6) have been tabulated in Table 9.

Steric accessibility of pathways was determined with the help of a zeolite visualization package. It was assumed that the proton would lie in the TOT plane as spanned by the T-sites and O atoms of the all-silica framework. Pathways were assumed to be accessible if the proton positions thus defined pointed into the same channel region. This method is considered to provide a good estimate in all but those few cases where the proton position was uncertain, as the TOT angle was close to 180°.

A total of 45 different sterically accessible pathways were identified. For 5 of the 12 crystallographically distinct T-sites we counted a maximum of five different paths per T-site. This occurs when two faces of the AlO_4 tetrahedron face different channels or when two faces are on the edge of the sinusoidal channel along the crystallographic *c*-axis. For one T-site by contrast, only one accessible path was found. The accessible paths are listed in Table 10.

One may note from the table that the paths that are energetically favorable (*i.e.*, between sites of lowest proton energy) are invariably sterically forbidden. This is because sites of low proton energy tend to lie in the interior of the MFI framework rather than on the large pores of the structure. This structure–property relationship was found in our previous study[6] and is now observed to affect catalytic behavior.

In the same manner as for FAU, we can calculate $\mathcal{F}_{MFI}$ by averaging over T-sites and over sterically accessible pathways. Using values of 0.6 and 0.8 eV for the width of the proton affinity distribution—as recommended in our earlier work[6]—we find that $\mathcal{F}_{MFI}$ varies with temperature between 0.054 (350 °C) and 0.094 (480 °C), and between 0.023 and 0.044, respectively. This is between 3 and 8 times as much as $\mathcal{F}_{FAU}$. Hence, we

Table 8. Proton Energies in FAU Relative to the Protonation Energy of Site 1[a]

site	proton energy (eV)
O_1	0
O_2	0.36 ± 0.03
O_3	-0.36 ± 0.15
O_4	0.56 ± 0.07

[a] Values and estimated errors are based on the averaging between predictions with four different force fields in ref 6.

Table 9. Estimated Energies of All Possible AlOH Combinations in MFI[a]

T-site	O-site	$\mathcal{E}$	T-site	O-site	$\mathcal{E}$
1	1	0.268	7	7	0.220
	15	0.691		17	−0.494
	16	−1.723		22	0.134
	21	0.865		23	1.276
2	1	0.238	8	7	0.259
	2	1.581		8	0.628
	6	−0.705		12	−1.665
	13	−1.183		13	−0.866
3	2	1.619	9	8	0.406
	3	−0.879		9	−1.199
	19	−0.910		18	1.082
	20	0.628		25	0.627
4	3	−0.752	10	9	−1.459
	4	0.616		10	−0.824
	16	−1.293		15	0.994
	17	−0.139		26	0.750
5	4	0.284	11	10	−0.899
	5	1.016		11	0.399
	14	−0.761		14	−0.350
	21	0.973		22	0.291
6	5	1.042	12	11	0.074
	6	−1.095		12	−1.864
	18	0.991		20	0.784
	19	−0.943		24	1.313

[a] Taken from the study in ref 6, where the data were presented in graphical form.

(28) Jirák, Z.; Vratislav, V.; Bosáček, V. *Phys. Chem. Solids* **1980**, *41*, 1089.

(29) Olsen, D. H.; Kokotailo, G. T.; Lawton, S. L.; Meier, W. M. *J. Chem. Phys.* **1981**, *85*, 2238.

Table 10. Sterically Accessible Pathways for D/H Exchange with Methane in MFI[a]

T-site	$O_i \leftrightarrow O_j$	T-site	$O_i \leftrightarrow O_j$
1	1 ↔ 15	7	7 ↔ 22
1	1 ↔ 21	7	7 ↔ 23
1	15 ↔ 21	7	17 ↔ 23
2	1 ↔ 2	7	22 ↔ 23
2	1 ↔ 6	8	7 ↔ 8
2	1 ↔ 13	8	7 ↔ 13
2	2 ↔ 6	8	8 ↔ 13
2	2 ↔ 13	9	8 ↔ 18
3	2 ↔ 3	9	8 ↔ 25
3	2 ↔ 19	9	9 ↔ 18
3	3 ↔ 20	9	9 ↔ 25
3	3 ↔ 20	9	18 ↔ 25
3	19 ↔ 20	10	9 ↔ 15
4	3 ↔ 4	10	9 ↔ 26
4	3 ↔ 17	10	15 ↔ 26
4	4 ↔ 17	11	11 ↔ 22
5	4 ↔ 5	12	11 ↔ 20
5	4 ↔ 21	12	11 ↔ 24
5	5 ↔ 14	12	20 ↔ 24
5	5 ↔ 21		
5	14 ↔ 21		
6	5 ↔ 6		
6	5 ↔ 18		
6	5 ↔ 19		
6	6 ↔ 18		
6	18 ↔ 19		

[a] The results are based on optical inspection of the three-dimensional structure. The numbers refer to the structure determination of Olson *et al.*[29]

have

$$\frac{r_f(\mathrm{MFI})}{r_f(\mathrm{FAU})} = \frac{\mathcal{F}_{\mathrm{MFI}}}{\mathcal{F}_{\mathrm{FAU}}} \approx 5 \pm 2 \qquad (33)$$

as a final result.

The main source of uncertainty in this predicted activity ratio is the uncertainty of proton energies. An independent theoretical estimate of proton energies in the zeolites FAU and MFI has been published by Sauer and co-workers.[4,5] Using their results, we find a value for $\mathcal{F}_{\mathrm{MFI}}/\mathcal{F}_{\mathrm{FAU}}$ of 4(±2). The somewhat lower value reflects the lower spread in proton energies found by these authors.

It is interesting to note that the higher activity of MFI is essentially due to the larger number of crystallographically independent T-sites (12 for MFI vs 1 for FAU). Figure 8 shows the site-dependence of the activity in both zeolites. In FAU the one T-site has about "average" activity, whereas in MFI a range of activities is observed, of which the most active determine the overall activity.

5. Comparison with Experiments

Previously, we presented an outline of the theoretical results together with new experimental data to test the predictions.[14] Since the focus here is on theory, we will only briefly review the comparison with experiment.

D/H exchange between deuterated methane and H-zeolites (Si:Al > 10) was monitored by measuring the time-evolution of the infrared adsorption spectrum of a closed container of zeolite in contact with an excess amount of methane at a constant pressure of 13 Torr. Over time, the absorption intensity of the stretch vibration of acid OH (I_{OH}) was observed to disappear exponentially

$$I_{OH}(t) = I^0_{OH} \exp(-t/\tau) \qquad (34)$$

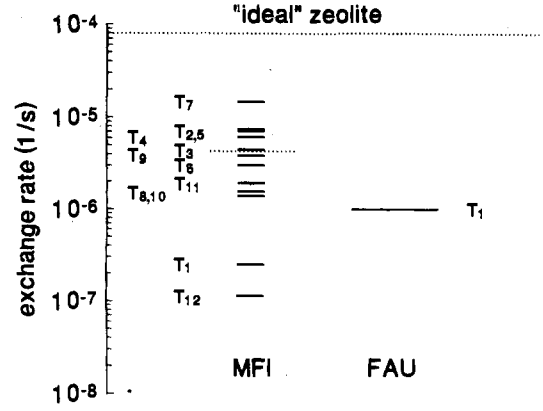

Figure 8. Calculated reaction rate (per Al site) for the D/H exchange of CD_4 and zeolites FAU and MFI, with respect to that of an "ideal" zeolite at 440 °C and 13 Torr CD_4 pressure. The site-dependent activity levels for FAU and MFI are scaled to the experimentally observed, average activity (dotted lines). For FAU the averaging is between accessible and inaccessible protons.

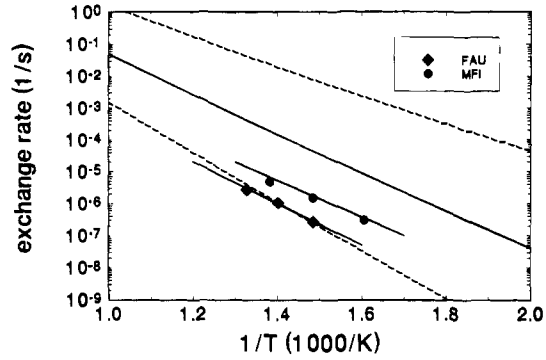

Figure 9. Experimental and theoretical D/H exchange rates in the zeolites FAU and MFI. Experimental data are taken from Kramer *et al.*.[14] The uncertainty in the absolute value of the barrier B_0 (1.6 ± 0.3 eV) is indicated by the dashed lines and holds for the "ideal zeolite". The line through the data points is obtained using the central value (1.6 eV) for the barrier B_0 multiplied by the appropriate correction factors $\mathcal{F}$ as calculated in section 4.

where τ is related to the reaction rate r_f

$$\tau = \frac{r_f}{[\mathrm{HZ}]} \qquad (35)$$

The decay time τ was measured at different temperatures between 350 and 480 °C. The temperature range is limited on the low-temperature side by the experimentalist's patience and on the high-temperature side by the onset of pyrolysis of methane, which can cause interferences at temperatures exceeding 500 °C.

Figure 9 shows the experimentally observed τ for H-zeolites FAU and MFI, together with our predictions from transition state theory, as well as the exchange rate for the hypothetical "ideal zeolite". For the latter, the uncertainty due to the inaccuracy of the value for B^0_0 is also indicated. The values at experimentally accessible temperatures coincide satisfactorily with the theoretical predictions. The large uncertainty in the absolute reaction rate does not invalidate our conclusion about the much smaller difference between FAU and MFI, since the uncertainty in B^0_0 affects the predictions for both zeolites identically.

The theoretical comparison between FAU and MFI relies on force field estimates for proton affinity differences between crystallographically distinct sites. The uncertainty of these, and

especially those for MFI, is difficult to assess.[6] However, the higher activity of MFI, relative to FAU, is a robust result, relying essentially only on the difference in the number of crystallographically different T-sites and the width of the proton affinity distribution. Furthermore, it is consistent with experiments on other acid-catalysed reactions that produce the same ordering (see, *e.g.*, ref 30). The quantitative analysis of experimental exchange activity differences leads to an estimate for the differences in proton affinities in zeolites that is between 0.5 and 1 eV.

6. Conclusion

We have studied in detail the D/H exchange reaction between deuterated methane and the H-forms of the zeolites FAU (HY) and MFI (HZSM-5). The problem was approached from two different perspectives. Starting from the molecular side, we used accurate *ab initio* calculations to studfy the reaction between methane and a molecular zeolite cluster. Perturbation of these clusters could be used to assess the effects of the heterogeneity of proton affinity (acidity) between different sites in a zeolite. We then estimated these proton affinity differences for FAU and MFI by means of force field calculations on periodic lattices. Combining both, we were able to predict both the reaction rate itself as well as the difference in reaction rates between these two zeolites. It was found that the reaction rate is determined by *differences* in acidity between the two oxygen sites involved in the exchange process, and the *absolute* acidity does not play a role. Finally, the theoretical results compare favorably with experimental data, showing that with present day computational capabilities it is possible to shed light on zeolite-catalyzed reactions.

Acknowledgment. The authors acknowledge the helpful discussions with Drs. C. A. Emeis, A. K. Nowak, and A. M. Rigby.

JA941374T

(30) Xu, T.; Munson, E. J.; Haw, J. F. *J. Am. Chem. Soc.* **1994**, *116*, 1962.